Stepwise unfolding supports a subunit model for vertebrate kinetochores

Stepwise unfolding supports a subunit model for vertebrate kinetochores

Giulia Vargiu[1], Alexandr A. Makarov[1], James Allan[2], Tatsuo Fukagawa[3], Daniel G. Booth[1‡] and William C. Earnshaw[1‡]

[1]Wellcome Trust Centre for Cell Biology
University of Edinburgh, King's Buildings, Max Born Crescent
Edinburgh EH9 3BF, Scotland, UK

[2]MRC Human Genetics Unit, Institute of Genetics and Molecular Medicine
The University of Edinburgh
Edinburgh EH4 2XU, Scotland, UK

[3]Laboratory of Chromosome Biology
Graduate School of Frontier Biosciences
Osaka University
Suita, Osaka 565-0871
JAPAN

‡Corresponding authors
bill.earnshaw@ed.ac.uk
daniel.booth@ed.ac.uk

ABSTRACT

During cell division, interactions between microtubules and chromosomes are mediated by the kinetochore, a proteinaceous structure located at the primary constriction of chromosomes. In addition to the centromere histone CENP-A, 15 other members of the Constitutive Centromere Associated Network (CCAN), participate in the formation of a chromatin-associated scaffold that supports kinetochore structure. We performed a targeted screen analysing unfolded centrochromatin from centromere protein (CENP) depleted chromosomes. Our results revealed that CENP-C and CENP-S are critical for the stable folding of mitotic kinetochore chromatin. Multi-peak fitting algorithms revealed the presence of an organised pattern of centrochromatin packing consistent with arrangement of CENP-A containing nucleosomes into up to five chromatin “subunits” – each containing roughly 20-30 nucleosomes. These subunits could be either layers of a boustrophedon or small loops of centromeric chromatin.

Significant statement

During cell division, microtubules apply pico-newton forces to segregate duplicated chromosomes into daughter cells. The kinetochore, located on the surface of the centromere chromatin, couples microtubules to the chromosomes. Little is known about the folding of the centromeric chromatin and how this templates the functional ultrastructure of the kinetochore. To better understand this fundamental problem, we used a microscopy technique that allowed the DNA associated with centromeric chromatin to be unfolded and accurately measured in the presence and absence of several key kinetochore components. By combining this microscopy method with statistical analysis of the unfolded chromatin fibres, we acquired data that allowed a subunit model of the kinetochore chromatin to be proposed.

\body

INTRODUCTION

The centromere is the genetic locus located at the primary constriction of mitotic chromosomes that directs chromosome segregation. Biochemically, the centromere is defined by the presence of the histone H3 variant CENP-A (1, 2) interspersed with canonical H3 nucleosomes carrying active chromatin marks (3, 4). This specialised chromatin class has been termed 'centrochromatin' (5). During cell division, an elaborate multi-subunit protein superstructure, the kinetochore, assembles on the surface of the centrochromatin to direct chromosome segregation.

Kinetochores contain ≥100 different proteins, 16 of which comprise the constitutive centromere associated network (CCAN). The CCAN remains associated with centromeric chromatin across the entire cell cycle (6-8). The CCAN includes CENP-A, CENP-C and three multi-subunit complexes: CENP-L/-N (9); CENP-H/-I/-K/-M (10); CENP-0/-P/Q-/R/-U (11) and CENP-T/-W/-S/-X (12-15).

Although numerous immuno-electron microscopy (16-18) and super-resolution microscopy (19-21) studies have mapped the locations of CCAN components relative to one another, the packing of the chromatin fibre in centrochromatin remains unknown. Early studies of stretched chromosomes suggested a repeating "subunit" structure for the kinetochore (1, 22). One subsequent hypothesis was that centrochromatin is composed of "amphipathic" helices or loops, with CENP-A-containing nucleosomes facing the outer kinetochore and H3 chromatin oriented towards the interior (5). A recent study proposed that centrochromatin is folded back and forth into a sinusoidal patch or

58 boustrophedon with a multi-layered structure stabilized during mitosis
59 by CENP-C (4).
60 Here, we have dissected centrochromatin organisation by
61 progressively unfolding the chromatin at low ionic strength in lysed
62 interphase and mitotic cells. Measurement of the lengths of the
63 resulting fibres revealed that centrochromatin unfolds in a series of
64 discrete (~ 0.5 μm) steps, consistent with a repeat substructure. CENP-C
65 and CENP-S separately contribute to the stability of the centrochromatin
66 structure during mitosis.
67

RESULTS AND DISCUSSION

Step-wise unfolding of CENP-A centrochromatin

To characterise the folding of centromeric chromatin, we exploited the ability of low salt TEEN buffer, which lacks divalent cations (see Methods) to unravel highly compact kinetochore chromatin into extended fibres (23) (Fig. 1A). To identify unfolded centromeric regions we generated cells expressing GFP:CENP-A from a DT40 wild type cell line. Expression of exogenous GFP:CENP-A had no effect on endogenous CENP-A levels (Fig. S1A). Furthermore, GFP:CENP-A was not present on chromosome arms (Fig. S1B), a potential artefact associated with CENP-A overexpression. GFP:CENP-A was found exclusively at the kinetochore, co-localising with CENP-T, at all cell cycle stages (Fig. S1B) - even on unfolded centrochromatin (Fig. S1C). This cell line was used to analyse centromere unfolding in both interphase and mitotic cells (Fig. 1B).

We used correlative light and electron microscopy (CLEM) to determine the extent of chromatin unfolding induced by TEEN treatment. A line-scan analysis of correlative EM images confirmed the presence of fibres with a mean diameter of 12.6 ± 2.19 nm, consistent with the diameter of a single chromatin fibre (Fig. 1C). Thus, TEEN treatment can unfold chromatin to the level of single fibres.

Collective analysis of >1300 individual centrochromatin fibres revealed that interphase prekinetochores unfolded to a significantly greater extent than mitotic kinetochores (unfolded length of CENP-A domain - 1.664 ± 0.049 μm versus 0.936 ± 0.025 μm [median ± SEM] respectively, Fig. 1D). The increased stability presumably allows mitotic kinetochores to resist forces applied by spindle microtubules during chromosome movements.

To confirm that only single centromeres were analysed we measured GFP:CENP-A fluorescence levels as a function of chromatin fibre length (Fig. 1E). Total GFP:CENP-A amounts remained constant across a range of fibre lengths up to 2.5 μm (mean = 32240.46 ± 3872.53). This strongly suggests that each unfolded CENP-A "subunit" analysed consists of a single unfolded centromere.

To determine whether centromeres unfold at random or in discrete steps, we analysed the distribution of unfolded fiber lengths using frequency histograms and multi-peak fitting algorithms to reveal periodicities in the data. Our comprehensive datasets (>650 measurements per sample) allowed us to generate high-resolution histograms (100 x 0.1 μm bins). This revealed the apparent presence of sub-populations of unfolded fibres, an observation masked with coarser bin widths (Fig. S2A). We then defined the periodicities observed (Fig. S2B), using the multi-peak fitting software Igor Pro 6.2 (WaveMetrics, Inc.) (see Methods). Five distinct peaks were recognised in interphase unfolded centrochromatin (Fig. 2A) and only three peaks in its mitotic counterpart (Fig. 2B). Each peak represented a node of accumulation of subpopulations of fibres, each corresponding to a potential "subunit" of centrochromatin released from the kinetochore.

To estimate the amount of DNA present in each unfolding "subunit" we determined the density of nucleosome packing in mitotic chromatin fibres unfolded under these conditions by analysing TEM of chromosome spreads prepared in TEEN buffer. The average center-to-center distance between adjacent nucleosomes was 20.43 ± 0.68 nm (Fig. S3A). The comparable distance from chicken erythrocyte interphase chromatin in low salt buffer was 38.71 ± 1.6 nm (Fig. S3B). These

numbers could not be measured specifically at centromeres, and thus provide only baseline values for estimating the chromatin packing.

Having measured peak locations and an approximate internucleosome distance we could estimate the amount of DNA present within the kinetochore. The distance between the fibre origin, the first peak, and pairs of adjacent peaks (steps) were interpreted as measures of chromatin length per unfolding "subunit". Interphase fibres unfolded in 5 steps with a mean step size of 0.69 ± 0.24 µm (Fig. 3A). Assuming 200 bp per average nucleosome, this corresponds to 17.8 Kbp of DNA (Fig. S3C). In mitosis, we identified three more variable steps (0.83 ± 0.33 µm) corresponding to roughly 24.4 Kbp of chromatin (Figs. 3B, S3C). These estimates of DNA content assume that the centrochromatin unfolds completely and are therefore almost certainly underestimates.

If we exclude the first step, subsequent steps of unfolding of interphase chromatin are remarkably reproducible, with a step size of 0.58 ± 0.1 µm, corresponding to roughly 15 nucleosomes (Fig. 3A). Interestingly, the first step is almost exactly twice this. A similar consideration of the mitotic unfolding is more speculative, given the apparent variable spacing and small number of steps. However, the minimum observed step (0.45 µm – ~22 nucleosomes), is close to the average step size observed for interphase chromatin, and again, almost exactly half the length of the first step.

Remarkably, a recent paper looking at human centromeres calculated that 1 in 25 centromeric nucleosomes contains CENP-A (24). Although the corresponding measurements have not been made for DT40 cells, the correlation with the average "subunit" size measured

here is striking. It is therefore possible that each centrochromatin "subunit" is organised around a single CENP-A nucleosome in DT40 cells.

It is tempting to speculate that unfolding of centrochromatin in low ionic strength buffer begins for interphase chromatin with two "subunits", followed by four individual steps, and in mitotic chromatin with two steps of one single "subunit". The differences in total length suggest either that the CENP-A chromatin domain is smaller in mitosis compared to interphase or (more likely) that the mitotic chromatin is more constrained and unfolds only partly.

What are the "subunits" likely to be? Given that they correspond to roughly 20-30 nucleosomes, we suggest that it is unlikely that they would correspond to gyres of a chromatin helix (Fig. 4A). The solenoid as described by Finch and Klug was proposed to have from 4 to 10 subunits per turn (25), and increasing this 2 or 3-fold would give rise to chromatin fibres much wider than typically seen. They could, however, correspond to folded loops (Fig. 4B) or to successive layers of a boustrophedon (a stack of planar sinusoidal patches) (Fig. 4C) (4). Interestingly, the typical width of a kinetochore plate measured by electron microscopy in DT40 cells is 227 nm (26). This would easily accommodate layers containing 25 nucleosomes inter-linked by other components of the CCAN.

The role of CCAN proteins in the maintenance of kinetochore chromatin folding

To further dissect the role of individual CCAN components in stabilising "subunit" interactions in centrochromatin, we analysed fibre unfolding following the depletion of specific CENPs. This analysis used conditional knockouts (designated GENENAME$^{ON/OFF}$) for CENP-C; CENP-

H, CENP-I (from the CENP-H/-I/-K/-M complex); CENP-N (from the CENP-L /-N complex); CENP-T/-W (from the CENP-T/-W/-S/-X complex); Ndc80 (from the Ndc80 complex); and absolute knockouts (designated GENENAME^{KO}) for the non-essential proteins CENP-S and CENP-O (from the CENP-O/-P/-Q/-R/-U complex). Generation of these knockout cell lines was previously described (4, 7, 14, 26-32). We confirmed that the growth properties of each cell line remained as previously described for the original knockouts (Figs. S4B, S5B).

Each mutant cell line was engineered to stably express GFP:CENP-A. GFP:CENP-A colocalized with CENP-T at centromeres both in the presence or absence of doxycycline (Fig. S4A). CENP-T localization was decreased following CENP-H and CENP-I depletion and abolished in CENP-N, CENP-T and CENP-W mutants (Fig. S5A). Immunoblotting analysis showed some variability in the expression levels of the total CENP-A across the cell lines (Figs. S4C, S5C, S6).

To examine the role of individual proteins in the stability of mitotic kinetochore chromatin, cells were depleted of target proteins (+dox or +aux) and synchronized in mitosis, before processing for fibre analysis. A striking difference in the median unfolded length was seen between mitotic centrochromatin fibres from wild type (0.936 ± 0.025 µm) and both CENP-C^{OFF} (2.207 ± 0.135 µm) and CENP-S^{KO} (1.66 ± 0.143 µm) cells (Fig. 5A). Strikingly, CENP-C depletion resulted in an even greater extension of the mitotic centromere than was seen with wild type interphase fibres (1.664 µm ± 0.049; $p<0.0001$) (Fig. 5A).

Small, albeit statistically significant changes were also observed following the depletion of CENP-H, CENP-T, CENP-I and CENP-N (Fig. 5A). These effects are small, and in an earlier, less extensive, study depletion

of CENP-H appeared not to affect the stability of the mitotic kinetochore (4). No destabilization was observed for mitotic centrochromatin fibres from CENP-O^{KO}, Ndc80^{OFF} or CENP-W^{OFF} cells.

Analysis of the unfolding step sizes for mitotic centrochromatin, revealed the existence of two classes of mutants (Figs. 3, S7, S8). The first, composed of CENP-H^{OFF}, CENP-I^{OFF}, Ndc80^{OFF}, CENP-O^{KO}, CENP-N^{OFF}, CENP-W^{OFF} and CENP-T^{AID} cells (Figs. 3, S7, S8), showed a mean unfolding step of 0.49 ± 0.05 μm (compared to 0.45 μm for wild type mitotic centrochromatin), which was preceded by a mean step of 0.76 ± 0.04 μm (0.81 μm in wild type). No third step was seen in these samples, possibly due to the decreased sample size, as that step corresponded to only 3% of unfolded kinetochore fibres from mitotic wild type cells. These data reveal that mitotic centrochromatin from CENP-H^{OFF}, CENP-I^{OFF}, Ndc80^{OFF}, CENP-O^{KO}, CENP-N^{OFF}, CENP-W^{OFF} and CENP-T^{AID} cells apparently unfolds like wild type centrochromatin. Therefore, these kinetochore components play at most a minor role in stabilising the mitotic kinetochore chromatin packing as detected by this assay.

In contrast, the unfolding pattern exhibited by centrochromatin from CENP-C^{OFF} and CENP-S^{KO} cells was very different from that seen with either wild type or the other mutants (Figs. 3, S7). Unfolding involved four steps instead of the three seen in wild type, and in contrast to the other examples, the unfolding proceeded in relatively equal steps (i.e. not two “subunits” followed by one). Furthermore, each step was roughly twice the length of the minimum step seen for wild type. Thus, mitotic centrochromatin from CENP-C^{OFF} and CENP-S^{KO} cells unfolded with a mean step size of 1.172 ± 0.12 μm and 1.110 ± 0.08 μm, respectively (Fig. 3C, D). This is consistent with a model where CENP-C

and CENP-S are required to link adjacent centrochromatin “subunits” (e.g. loops or layers of a boustrophedon) together.

In addition to the different step size, unfolded centrochromatin fibres from CENP-S^{KO} and CENP-C^{OFF} cells average 1.8 - 2.4 – times longer than the corresponding fibres from wild type (Fig. 5A). Thus, in addition to causing a different pattern of unfolding, the loss of CENP-C and CENP-S also results in a greater overall extent of kinetochore unfolding. This reinforces the conclusion that the organisation of the kinetochore chromatin in these mutant cells is significantly different from that in wild type.

Importantly, interphase centrochromatin from CENP-C^{OFF} and CENP-S^{KO} cells behaves very differently (Fig. 5B). CENP-C^{OFF} interphase centrochromatin unfolds to the same extent as wild type, but CENP-S^{KO} interphase centrochromatin unfolds to a significantly greater extent. This strongly suggests that even though both proteins are required for the stabilisation of centrochromatin, they may do so via distinct mechanisms.

Our data support previous conclusions that the inner kinetochore protein CENP-C (17, 20), forms a nexus for multiple interactions that stabilise the mitotic kinetochore, amongst other things, determining the diameter of the outer kinetochore plate (33). Indeed, CENP-C is required to efficiently recruit both inner and outer kinetochore components during kinetochore assembly (34-37).

The destabilization of mitotic kinetochores in CENP-S^{KO} cells was surprising. CENP-S is part of the hetero-tetrameric CENP-T/-W/-S/-X complex (12). However, loss of CENP-W had no effect and CENP-T only a minor effect on centrochromatin stability in our assay. Detectable

(though reduced) levels of CENP-T are retained at kinetochores of CENP-S^{KO} cells, and chromosomes appear to contain both CENP-T/-W and CENP-T/-W/-S/-X complexes (37) (Fig. S4A). Similarly to CENP-C, an electron microscopy study reported that CENP-S depletion could affect kinetochore plate size (26).

Consistent with these effects on kinetochore plate size, quantitation of immunoblots revealed that the total CENP-A levels were lowest in CENP-C^{OFF} and CENP-S^{KO} cell lines (Fig. S6). However human cells normally contain excess CENP-A molecules (24), and chicken cells survive up to 4 days following CENP-A depletion, by which time CENP-A molecules have been diluted 12-fold (38). The lower level of CENP-A is unlikely to explain the centrochromatin destabilization in those mutants since there is very little difference in total CENP-A levels between CENP-C^{OFF} and CENP-I^{OFF} cells even though the centrochromatin is destabilized in one and normal in the other.

Possible roles of CENP-S at the kinetochore are complicated by the fact that this protein also functions in DNA repair. CENP-S/MHF1 has a role in the resolution of DNA interstrand crosslinks and sister chromatid exchanges (SCEs) by the Fanconi Anemia complex. CENP-S is required for chromatin targeting and stability of the FANCM subcomplex, of which it is a member together with CENP-X/MHF2 (39, 40). In DT40 cells, SCEs increased 3-4 fold when CENP-S/MHF1 was depleted (39, 40). Thus, CENP-S involvement in centrochromatin stability may reflect a more general role in chromatin higher-order structure across the cell cycle.

Our results suggest that CENP-H/-I/-K/-M and Ndc80 complexes act within individual centrochromatin subunits, or between subunits and non-chromatin components of the kinetochore. In contrast, CENP-C has

a web of interactions with other CCAN members, including CENP-A and CENP-H/-I/-K/-M (35, 36, 41) as well as outer kinetochore components (10, 42). CENP-T/W/S/X also interacts both with CENP-H/-I/-K/-M (10) and the Ndc80 complex (13, 43). We considered whether interactions between the inner and outer kinetochore might stabilise mitotic centrochromatin, but this is unlikely, as kinetochores lacking Ndc80 have a "subunit" organisation and mitotic stability similar to wild type (Figs. 3H, 5A).

The dependencies on centrochromatin stability observed here do not appear to correspond to the recent description of "core" and "expandable" kinetochore modules described recently in Xenopus extracts (44). There, CENP-A, CENP-H/-I/-K/-M, CENP-T/W/S/X and Ndc80 were all found to part of the "core" kinetochore that was unaffected by the loss of microtubules, whereas CENP-C was involved in the expansion that occurred when microtubules were absent. The authors suggested that this expansion did not involve the centrochromatin, but rather corresponded to a polymerization of protein complexes, in which the multifunctional CENP-C played a key role. This is consistent with our observation that both a "core" component (CENP-S) and an "expandable" component (CENP-C) are involved in mitotic centrochromatin stability.

The role of CENP-O/-P/-Q/-R/-U in kinetochore organisation remains enigmatic. Studies in *S. cerevisiae* report a role for the COMA complex (CENP-O/-P/-Q/-R/-U complex homolog) in the looping of centromere chromatin (45). However our results plus other recent studies have failed to identify a function for this complex in vertebrate kinetochores (37, 41).

311 Given the measurements of internucleosome distance in bulk
312 chromatin of mitotic chromosomes and interphase nuclei unfolded in
313 low salt buffer (23), we estimated the amount of DNA present at
314 kinetochores in the different cell lines. According to the lengths
315 measured for CENP-A fibres, these values ranged of 12 to 45 Kbp. The
316 smaller number likely corresponds to fibres that were not completely
317 unfolded, whereas the larger number (from unfolded CENP-C^{OFF} and
318 CENP-S^{KO} chromosomes) was remarkably close to the estimated 50-60
319 kb of DNA in chicken kinetochores determined by quantitative
320 fluorescence microscopy (46), and the ~ 40 kb of DNA occupied by
321 CENP-A in chicken non-repetitive centromeres and neocentromeres,
322 determined by ChIP (47).
323 In the future, it will be important to devise super-resolution
324 imaging strategies in which a centrochromatin fibre can be traced in
325 intact mitotic chromosomes. A recent study revealed that kinetochores
326 form large crescents during early prometaphase when they are
327 "searching" for microtubules, and become more compact structures
328 once the attachments have matured (48). This raises an extremely
329 interesting fundamental question of whether the underlying chromatin
330 reorganization also changes at this time.
331

MATERIALS AND METHODS

Detailed electron microscopy procedures are described in the SI Materials and Methods.

Fibre length preparation and length measurements

Chromatin fibres were prepared using TEEN buffer (10 mM Triethanolamine:HCl pH 8.0, 10 mM NaCl, 5 mM EDTA) using an optimised version of a previously described method (49). GFP:CENP-A unfolded centrochromatin was imaged using a CCD camera (CoolSnap HQ, Photometrix) on a wide-field microscope (DeltaVision Spectris; Applied Precision) with a NA 1.4 Plan Apochromat 100X lens controlled by DeltaVision SoftWorx (Applied Precision). ImageJ (National Institute of Health, Bathesda, MD) segmented line tool was used to measure centromere chromatin fibre length.

Multi-peak analysis

Fibre unfolding data was imported in Igor Pro 6.2 (WaveMetrics, Inc.). Data sets were allotted into the appropriate number of histogram bins. The multi-peak fitting 2.0 package was used for peak identification using "Auto-Locate Peaks Now". This automatic peak finding algorithm searches for and identifies subpopulations by finding maxima in the smoothed second derivative of the data. To achieve this, the algorithm estimates both the noise level and optimum smoothing factor of the data. All adjustable parameters were kept within the same range across all samples: noise level 0.00005-0.06; smooth fraction 0.05-2.5; minimal fraction 0.035-0.5. After an initial estimation of the peaks the fitting algorithm was run and results were summarised in a table containing

information about peak location, area, type, amplitude and residuals. Residuals, or fitting deviations, represent the difference between the observed values with the predicted sample mean and the best fit curve. A positive value of residuals suggest that the measured value is placed above the best fitting curve whilst a negative one is referred to a value located underneath it. If the best fit curve passes through the value measured then the residuals equal zero. According to Igor Pro guidelines good fitting is achieved when deviation of the residuals is less then 0.1.

ACKNOWLEDGMENTS

This work was funded by The Wellcome Trust, of which WCE is a Principal Research Fellow [grant number 107022]. The Wellcome Trust Centre for Cell Biology is supported by core grant numbers 077707 and 092076 and Wellcome Trust Multi User Equipment Grant (WT104915MA). This work was supported by JSPS KAKENHI Grant Number JP25221106 and JP15H05972 to TF. GV was supported by a studentship from the Darwin Trust of Edinburgh.

AUTHOR CONTRIBUTIONS

GV, Acquisition of the data, Analysis and interpretation of the data, Drafting and revising the article critically for important intellectual content; AAM, Acquisition of the data; JA, Acquisition of the data; TF, Contributed with essential reagents, Revising the article critically for important intellectual content, Final approval of the version to be published; DGB, Acquisition of the data, Analysis and interpretation of the data, Design, Revising the article critically for important intellectual content, Final approval of the version to be published; WCE, Conception and design, Analysis and interpretation of the data, Revising the article critically for important intellectual content, Final approval of the version to be published.

CONFLICT OF INTEREST

The authors declare that no competing interests exist.

References

1. Earnshaw WC & Rothfield N (1985) Identification of a Family of Human Centromere Proteins Using Autoimmune Sera from Patients with Scleroderma. *Chromosoma* 91(3-4):313-321.
2. Palmer DK, O'Day K, Trong HL, Charbonneau H, & Margolis RL (1991) Purification of the centromere-specific protein CENP-A and demonstration that it is a distinctive histone. *Proceedings of the National Academy of Sciences of the United States of America* 88(9):3734-3738.
3. Blower MD, Sullivan BA, & Karpen GH (2002) Conserved organization of centromeric chromatin in flies and humans. *Dev Cell* 2(3):319-330.
4. Ribeiro SA, Vagnarelli P, Dong Y, Hori T, McEwen BF*, et al.* (2010) A super-resolution map of the vertebrate kinetochore. *Proceedings of the National Academy of Sciences of the United States of America* 107(23):10484-10489.
5. Sullivan BA & Karpen GH (2004) Centromeric chromatin exhibits a histone modification pattern that is distinct from both euchromatin and heterochromatin. *Nature structural & molecular biology* 11(11):1076-1083.
6. Foltz DR, Jansen LE, Black BE, Bailey AO, Yates JR, 3rd*, et al.* (2006) The human CENP-A centromeric nucleosome-associated complex. *Nature cell biology* 8(5):458-469.
7. Okada M, Cheeseman IM, Hori T, Okawa K, McLeod IX*, et al.* (2006) The CENP-H-I complex is required for the efficient incorporation of newly synthesized CENP-A into centromeres. *Nature cell biology* 8(5):446-457.
8. Izuta H, Ikeno M, Suzuki N, Tomonaga T, Nozaki N*, et al.* (2006) Comprehensive analysis of the ICEN (Interphase Centromere Complex) components enriched in the CENP-A chromatin of human cells. *Genes to cells : devoted to molecular & cellular mechanisms* 11(6):673-684.
9. Hinshaw SM & Harrison SC (2013) An Iml3-Chl4 heterodimer links the core centromere to factors required for accurate chromosome segregation. *Cell reports* 5(1):29-36.
10. Basilico F, Maffini S, Weir JR, Prumbaum D, Rojas AM*, et al.* (2014) The pseudo GTPase CENP-M drives human kinetochore assembly. *eLife* 3:e02978.
11. Eskat A, Deng W, Hofmeister A, Rudolphi S, Emmerth S*, et al.* (2012) Step-wise assembly, maturation and dynamic behavior of the human CENP-P/O/R/Q/U kinetochore sub-complex. *PloS one* 7(9):e44717.
12. Nishino T, Takeuchi K, Gascoigne KE, Suzuki A, Hori T*, et al.* (2012) CENP-T-W-S-X forms a unique centromeric chromatin structure with a histone-like fold. *Cell* 148(3):487-501.
13. Schleiffer A, Maier M, Litos G, Lampert F, Hornung P*, et al.* (2012) CENP-T proteins are conserved centromere receptors of the Ndc80 complex. *Nature cell biology* 14(6):604-613.
14. Hori T, Amano M, Suzuki A, Backer CB, Welburn JP*, et al.* (2008) CCAN makes multiple contacts with centromeric DNA to provide distinct pathways to the outer kinetochore. *Cell* 135(6):1039-1052.

15. Dornblut C, Quinn N, Monajambashi S, Prendergast L, van Vuuren C*, et al.* (2014) A CENP-S/X complex assembles at the centromere in S and G2 phases of the human cell cycle. *Open biology* 4:130229.
16. Cooke CA, Bernat RL, & Earnshaw WC (1990) CENP-B: a major human centromere protein located beneath the kinetochore. *The Journal of cell biology* 110(5):1475-1488.
17. Saitoh H, Tomkiel J, Cooke CA, Ratrie H, 3rd, Maurer M*, et al.* (1992) CENP-C, an autoantigen in scleroderma, is a component of the human inner kinetochore plate. *Cell* 70(1):115-125.
18. Suzuki A, Hori T, Nishino T, Usukura J, Miyagi A*, et al.* (2011) Spindle microtubules generate tension-dependent changes in the distribution of inner kinetochore proteins. *The Journal of cell biology* 193(1):125-140.
19. Joglekar AP, Bloom K, & Salmon ED (2009) In vivo protein architecture of the eukaryotic kinetochore with nanometer scale accuracy. *Curr Biol* 19(8):694-699.
20. Wan X, O'Quinn RP, Pierce HL, Joglekar AP, Gall WE*, et al.* (2009) Protein architecture of the human kinetochore microtubule attachment site. *Cell* 137(4):672-684.
21. Suzuki A, Badger BL, Wan X, DeLuca JG, & Salmon ED (2014) The architecture of CCAN proteins creates a structural integrity to resist spindle forces and achieve proper Intrakinetochore stretch. *Dev Cell* 30(6):717-730.
22. Zinkowski RP, Meyne J, & Brinkley BR (1991) The centromere-kinetochore complex: a repeat subunit model. *The Journal of cell biology* 113(5):1091-1110.
23. Earnshaw WC & Laemmli UK (1983) Architecture of metaphase chromosomes and chromosome scaffolds. *The Journal of cell biology* 96(1):84-93.
24. Bodor DL, Mata JF, Sergeev M, David AF, Salimian KJ*, et al.* (2014) The quantitative architecture of centromeric chromatin. *eLife* 3:e02137.
25. Finch JT & Klug A (1976) Solenoidal model for superstructure in chromatin. *Proceedings of the National Academy of Sciences of the United States of America* 73(6):1897-1901.
26. Amano M, Suzuki A, Hori T, Backer C, Okawa K*, et al.* (2009) The CENP-S complex is essential for the stable assembly of outer kinetochore structure. *The Journal of cell biology* 186(2):173-182.
27. Fukagawa T, Mikami Y, Nishihashi A, Regnier V, Haraguchi T*, et al.* (2001) CENP-H, a constitutive centromere component, is required for centromere targeting of CENP-C in vertebrate cells. *The EMBO journal* 20(16):4603-4617.
28. Nishihashi A, Haraguchi T, Hiraoka Y, Ikemura T, Regnier V*, et al.* (2002) CENP-I is essential for centromere function in vertebrate cells. *Dev Cell* 2(4):463-476.
29. Hori T, Haraguchi T, Hiraoka Y, Kimura H, & Fukagawa T (2003) Dynamic behavior of Nuf2-Hec1 complex that localizes to the centrosome and centromere and is essential for mitotic progression in vertebrate cells. *Journal of cell science* 116(Pt 16):3347-3362.

30. Kwon MS, Hori T, Okada M, & Fukagawa T (2007) CENP-C is involved in chromosome segregation, mitotic checkpoint function, and kinetochore assembly. *Molecular biology of the cell* 18(6):2155-2168.
31. Hori T, Okada M, Maenaka K, & Fukagawa T (2008) CENP-O class proteins form a stable complex and are required for proper kinetochore function. *Molecular biology of the cell* 19(3):843-854.
32. Wood L, Booth DG, Vargiu G, Ohta S, deLima Alves F*, et al.* (2016) Auxin/AID versus conventional knockouts: distinguishing the roles of CENP-T/W in mitotic kinetochore assembly and stability. *Open biology* 6(1):150230.
33. Tomkiel J, Cooke CA, Saitoh H, Bernat RL, & Earnshaw WC (1994) CENP-C is required for maintaining proper kinetochore size and for a timely transition to anaphase. *The Journal of cell biology* 125(3):531-545.
34. Hori T, Shang WH, Takeuchi K, & Fukagawa T (2013) The CCAN recruits CENP-A to the centromere and forms the structural core for kinetochore assembly. *The Journal of cell biology* 200(1):45-60.
35. Nagpal H, Hori T, Furukawa A, Sugase K, Osakabe A*, et al.* (2015) Dynamic changes in CCAN organization through CENP-C during cell-cycle progression. *Molecular biology of the cell* 26(21):3768-3776.
36. Klare K, Weir JR, Basilico F, Zimniak T, Massimiliano L*, et al.* (2015) CENP-C is a blueprint for constitutive centromere-associated network assembly within human kinetochores. *The Journal of cell biology* 210(1):11-22.
37. Samejima I, Spanos C, Alves Fde L, Hori T, Perpelescu M*, et al.* (2015) Whole-proteome genetic analysis of dependencies in assembly of a vertebrate kinetochore. *The Journal of cell biology* 211(6):1141-1156.
38. Regnier V, Vagnarelli P, Fukagawa T, Zerjal T, Burns E*, et al.* (2005) CENP-A is required for accurate chromosome segregation and sustained kinetochore association of BubR1. *Molecular and cellular biology* 25(10):3967-3981.
39. Singh TR, Saro D, Ali AM, Zheng XF, Du CH*, et al.* (2010) MHF1-MHF2, a histone-fold-containing protein complex, participates in the Fanconi anemia pathway via FANCM. *Molecular cell* 37(6):879-886.
40. Yan Z, Delannoy M, Ling C, Daee D, Osman F*, et al.* (2010) A histone-fold complex and FANCM form a conserved DNA-remodeling complex to maintain genome stability. *Molecular cell* 37(6):865-878.
41. McKinley KL, Sekulic N, Guo LY, Tsinman T, Black BE*, et al.* (2015) The CENP-L-N Complex Forms a Critical Node in an Integrated Meshwork of Interactions at the Centromere-Kinetochore Interface. *Molecular cell* 60(6):886-898.
42. Przewloka MR, Venkei Z, Bolanos-Garcia VM, Debski J, Dadlez M*, et al.* (2011) CENP-C is a structural platform for kinetochore assembly. *Curr Biol* 21(5):399-405.
43. Nishino T, Rago F, Hori T, Tomii K, Cheeseman IM*, et al.* (2013) CENP-T provides a structural platform for outer kinetochore assembly. *The EMBO journal* 32(3):424-436.
44. Wynne DJ & Funabiki H (2015) Kinetochore function is controlled by a phospho-dependent coexpansion of inner and outer components. *The Journal of cell biology* 210(6):899-916.

45. Anderson M, Haase J, Yeh E, & Bloom K (2009) Function and assembly of DNA looping, clustering, and microtubule attachment complexes within a eukaryotic kinetochore. *Molecular biology of the cell* 20(19):4131-4139.
46. Ribeiro SA, Vagnarelli P, & Earnshaw WC (2014) DNA content of a functioning chicken kinetochore. *Chromosome Res* 22(1):7-13.
47. Shang WH, Hori T, Martins NM, Toyoda A, Misu S*, et al.* (2013) Chromosome engineering allows the efficient isolation of vertebrate neocentromeres. *Dev Cell* 24(6):635-648.
48. Magidson V, Paul R, Yang N, Ault JG, O'Connell CB*, et al.* (2015) Adaptive changes in the kinetochore architecture facilitate proper spindle assembly. *Nature cell biology* 17(9):1134-1144.
49. Hudson DF, Vagnarelli P, Gassmann R, & Earnshaw WC (2003) Condensin is required for nonhistone protein assembly and structural integrity of vertebrate mitotic chromosomes. *Dev Cell* 5(2):323-336.
50. Ribeiro SA, Gatlin JC, Dong Y, Joglekar A, Cameron L*, et al.* (2009) Condensin regulates the stiffness of vertebrate centromeres. *Molecular biology of the cell* 20(9):2371-2380.
51. Booth DG, Takagi M, Sanchez-Pulido L, Petfalski E, Vargiu G*, et al.* (2014) Ki-67 is a PP1-interacting protein that organises the mitotic chromosome periphery. *eLife* 3:e01641.
52. Allan J, Staynov DZ, & Gould H (1980) Reversible dissociation of linker histone from chromatin with preservation of internucleosomal repeat. *Proceedings of the National Academy of Sciences of the United States of America* 77(2):885-889.
53. Allan J, Harborne N, Rau DC, & Gould H (1982) Participation of core histone "tails" in the stabilization of the chromatin solenoid. *The Journal of cell biology* 93(2):285-297.

FIGURE LEGENDS

Figure 1: Unfolding of centromere chromatin in interphase versus mitotic samples. A. Schematic explaining the method employed to unfold chromatin using TEEN buffer. TEEN has a low salt concentration and contains EDTA as a divalent cation chelator. The excess of negative charges on the DNA and the hypotonic environment together cause cells to burst and the chromatin to unfold. **B**. Representative fluorescence micrographs of unfolded centrochromatin fibres, detected using GFP:CENP-A and DAPI. Bar, 1 μm. **C**. CLEM analysis of unfolded chromatin from asynchronous cells. DAPI and GFP:CENPA were used to identify typical unfolded fibres. The same regions were revisited using TEM. Bar, 50 nm. Fibres visualized by TEM were analysed using multiple line-scans (see representative line-scan in black (bar, 50 nm)) and pixel density measurements. The data was plotted in a line graph where the line profile represents an average of 5 line-scans with standard deviation. Vertical red lines mark the edges of electron dense regions (i.e. the width of the chromatin fibre). **D**. Box and whisker plots showing the median fibre length for interphase and mitotic samples; the height of the box defines the interquartile range, whiskers indicate the 10^{th} and 90^{th} percentile. Asterisks indicate statistical significance of differences in fibre length between interphase and mitosis ($P < 0.0001$; Mann-Whitney U test) where $n=655^{fibres}$ in total per each sample, over 3 independent experiments. **E**. Bar chart showing GFP:CENP-A total fluorescence plotted as a function of centromere length (n=50). A range of fibre lengths up to 2.5 μm were tested. Data are presented as mean ± SEM, with bins of 0.5 μm increments.

Figure 2: The centromere is composed of multiple dynamic chromatin layers. Multi-peak analysis using data sets of unfolded centromere chromatin fibres from interphase and mitotic samples. **A** and **B** show probability density histograms (white bars). X and Y axes show centromere fibre length (μm) and frequency, respectively. Data are allotted into 100 bins, each with a resolution of 100 nm per bin. Multi-peak fitting algorithm identified putative populations of fibre lengths within the data sets, depicted by discrete peaks (red lines). Best fitting curve is also shown (blue line) for both samples.

Figure 3: Quantification of the steps of unfolding. Schematic displaying the sub-populations of the peaks (▲, μm) and the distance of the interval between two consecutive peaks (μm). Data obtained from multi-peak fitting analysis in Fig. S7.

Figure 4: Comparison of models for centrochromatin structure. A. Solenoid in which CENP-A (red) and H3 (grey) nucleosomes are organized at centromeres into helical gyres (1 gyre per "subunit") or **B.** Loops clustered next to each other (1 loop per "subunit"). These two models were first proposed by (3). Gyres and loops diagrammed here could both generate unfolded fibres in presence of TEEN with an unfolded length of roughly 0.5 μm. **C.** Boustrophedon model consisting of a stack of planar sinusoidal patches (layers) of centrochromatin (1 layer is a subunit). As a response to TEEN buffer, single layers of the boustrophedon might unfold into chromatin fibres 0.5 μm long.

Figure 5: Unfolding of centromere chromatin in CENP mutants. A and **B** Box and whisker plots displaying the spread of the data sets of unfolded fibre length measured in: **A.** wild type and the indicated mutants, after being blocked in nocodazole; **B.** wild type and indicated mutants asynchronous cells. The height of the box defines the interquartile range, whiskers indicate the 10^{th} and 90^{th} percentile. The n number is specified in each box. **A.** Each conditional knockout cell line has been tested for significant difference against unfolded fibres from control interphase or control mitosis. Only statistically insignificant comparisons are shown in the graph (Mann-Whitney U test). **B**. Mann-Whitney U test was performed confirming statistically significant differences between the mutants and wild type fibres.

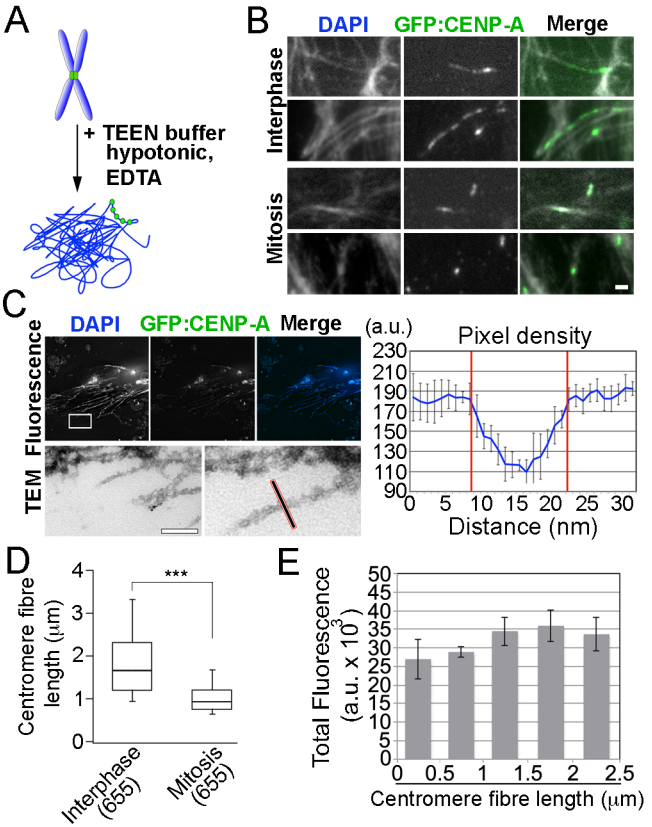
A
+ TEEN buffer
hypotonic,
EDTA
B
DAPI
GFP:CENP-A
Merge
Interphase
Mitosis
C
DAPI
GFP:CENP-A
Merge
Fluorescence
TEM
(a.u.)
Pixel density
230
210
190
170
150
130
110
90
0
5
10
15
20
25
30
Distance (nm)
D
Centromere fibre length (μm)
***
Interphase (655)
Mitosis (655)
E
Total Fluorescence (a.u. x 10^3)
Centromere fibre length (μm)

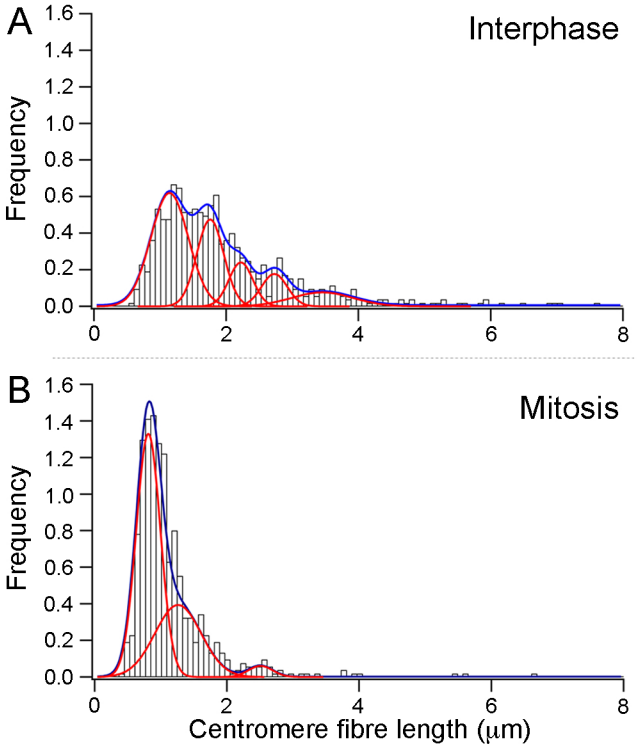
A
Interphase
Frequency
1.6
1.4
1.2
1.0
0.8
0.6
0.4
0.2
0.0
0
2
4
6
8

B
Mitosis
Frequency
1.6
1.4
1.2
1.0
0.8
0.6
0.4
0.2
0.0
0
2
4
6
8
Centromere fibre length (μm)

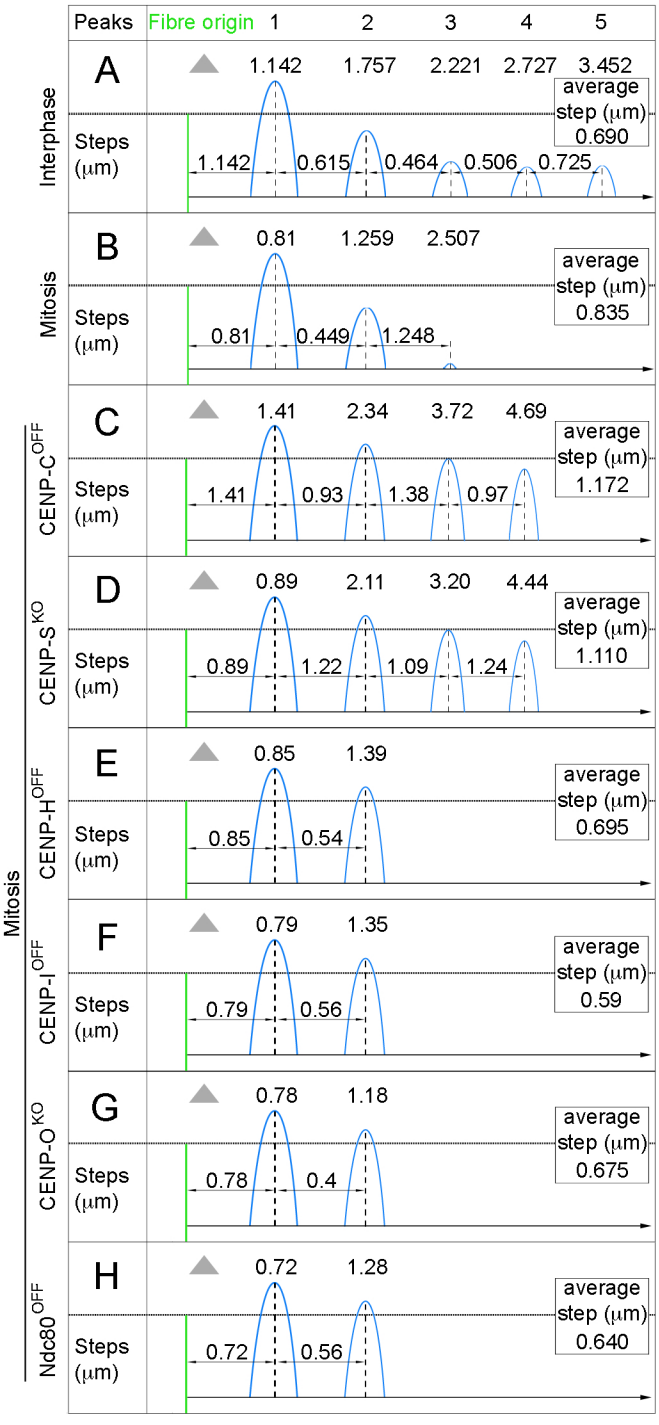
Peaks
Fibre origin
1
2
3
4
5
A
Interphase
1.142
1.757
2.221
2.727
3.452
average step (μm) 0.690
Steps (μm)
1.142
0.615
0.464
0.506
0.725
B
Mitosis
0.81
1.259
2.507
average step (μm) 0.835
Steps (μm)
0.81
0.449
1.248
Mitosis
C
CENP-C OFF
1.41
2.34
3.72
4.69
average step (μm) 1.172
Steps (μm)
1.41
0.93
1.38
0.97
D
CENP-S KO
0.89
2.11
3.20
4.44
average step (μm) 1.110
Steps (μm)
0.89
1.22
1.09
1.24
E
CENP-H OFF
0.85
1.39
average step (μm) 0.695
Steps (μm)
0.85
0.54
F
CENP-I OFF
0.79
1.35
average step (μm) 0.59
Steps (μm)
0.79
0.56
G
CENP-O KO
0.78
1.18
average step (μm) 0.675
Steps (μm)
0.78
0.4
H
Ndc80 OFF
0.72
1.28
average step (μm) 0.640
Steps (μm)
0.72
0.56

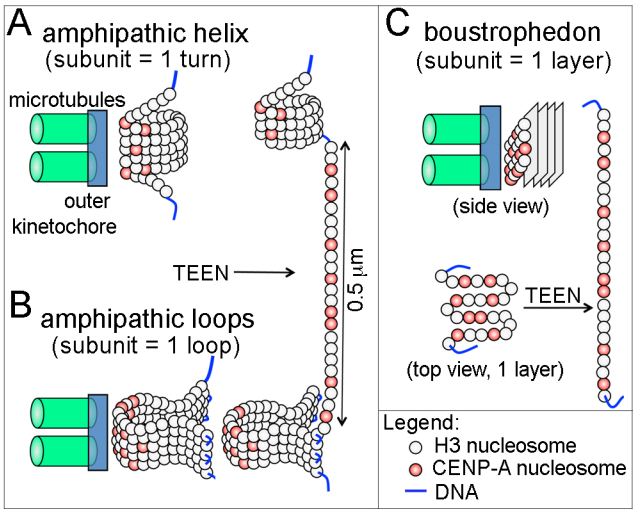
A amphipathic helix
(subunit = 1 turn)
microtubules
outer
kinetochore
TEEN
0.5 µm
B amphipathic loops
(subunit = 1 loop)
C boustrophedon
(subunit = 1 layer)
(side view)
TEEN
(top view, 1 layer)
Legend:
H3 nucleosome
CENP-A nucleosome
DNA

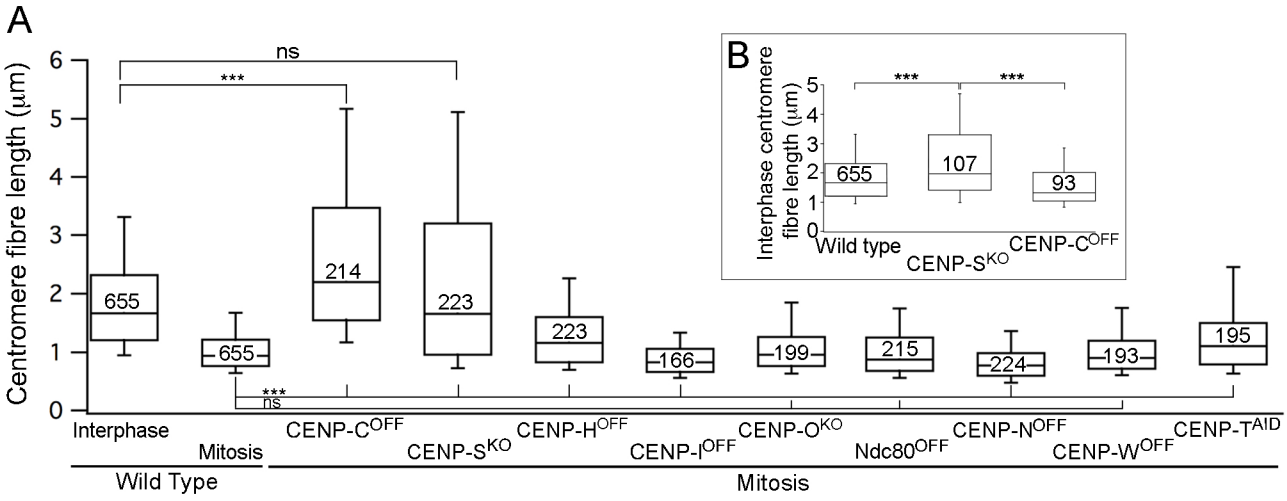
A
Centromere fibre length (μm)
0
1
2
3
4
5
6
ns
***
655
655
214
223
223
166
199
215
224
193
195
***
ns
Interphase
Mitosis
CENP-C^OFF
CENP-S^KO
CENP-H^OFF
CENP-I^OFF
CENP-O^KO
Ndc80^OFF
CENP-N^OFF
CENP-W^OFF
CENP-T^AID
Wild Type
Mitosis
B
Interphase centromere fibre length (μm)
0
1
2
3
4
5
***
***
655
107
93
Wild type
CENP-S^KO
CENP-C^OFF

SUPPLEMENTARY MATERIALS AND METHODS

Cell culture

Chicken B lymphoma DT40 cells were grown in RPMI 1640 medium supplemented with 10% FBS, 1% chicken serum and 1% penicillin/streptomycin at 39°C in 5% CO_2. CENP-C (30), CENP-H (27), CENP-I (28) and Ndc80 (29), CENP-T^{AID} (32) conditional knockout cell lines were transfected with GFP:GgCENP-A cloned in pEGFPC1 vector with 17-amino acid linker (50). Cell lines stably expressing GFP:GgCENP-A were obtained by co-electroporation with puromycin, hygromycin and geneticin-resistant markers. CENP-N and CENP-W conditional knockout cell lines stably expressing GFP:CENP-A were previously generated (4). The addition to the media of 500 ng/ml of doxycycline or auxin at the final concentration of 125 μM destroyed the expression of the rescuing cDNA. DT40 cells were blocked in mitosis by treating with 500 ng/ml nocodazole for 12 hours.

Cell vital counts using Trypan Blue

For cell counts experiments, 1 part of trypan blue was added to 1 part of cell suspension at room temperature. DT40 cells were maintained at a concentration of 20 X 10^4 cells/ml at each dilution time.

CENP-A total fluorescence quantification

For 50 fibres randomly picked images were deconvolved and projected into ImageJ (National Institute of Health, Bethesda, MD) and the area occupied by CENP-A signal along each fibre was highlighted by thresholding and then selected with the magic wand. The fluorescence,

measured in ImageJ, was annotated. Graphs were produced in Microsoft Excel.

Correlative light electron microscopy (CLEM) of unfolded fibres

The CLEM protocol was adapted from a previously established method (51). DT40 cells expressing GFP:CENPA were seeded onto ConA coated glass-bottomed gridded dishes (MatTeK Corporation, USA), and left to adhere for 1 hour. Fibres were prepared using the standard protocol until the point of fixation. Fibres were fixed for 1 hour with 3% glutaraldehyde and 0.5% formaldehyde in 0.2 M sodium cacodylate buffer containing 5 μg/mL Hoechst. Fibres were washed with PBS and imaged in PBS using a DeltaVision microscope (Applied Precision) where GFP:CENP-A centrochromatin was detected. Transmitted light was used to map cell positions via reference coordinates. The reference images allowed for the correlative re-identification of cells of interest by electron microscopy. DeltaVision acquisition was followed by treatment with tannic acid (0.1% in water) for 20 minutes, followed by osmication (1% osmium tetroxide in PBS) for 1 hour. Samples were then washed with PBS, ddH2O and 30% ethanol before the incubation in uranyl acetate (0.5% in 30% ethanol) for 1 hour. Next, fibres were dehydrated using a graded series of ethanol washes. Following dehydration, samples were infiltrated with ethonal:resin mixtures (2:1 and 1:1) for 20 minutes each. Finally, cells were embedded in 100% resin (TAAB), with a gelatin capsule of resin covering the cells of interest, before curing at 60 °C for 3 days. Polymerised resin blocks were sectioned and post stained as routine. Samples were viewed using a Phillips CM120 BioTwin

transmission electron microscope (FEI) and micrographs acquired using a Gatan Orius CCD camera (Gatan).

Electron microscopy of mitotic nucleosomes

Chromosomes isolated from colcemid arrested HeLa cells were centrifuged at 1,400 g for 20 minutes at 4°C onto carbon-coated grids and rinsed in 0.4% Photoflo (Kodak). Grids were fixed in TEEN buffer containing 1% glutaraldehyde for 1-2 hours at 4°C. Grids were consecutively dipped into 1% phosphotungstic acid in 71% ethanol (15 sec), 95% ethanol (15 sec), 0.4% Photoflo (5 sec), blotted dry and rotary shadowed using platinum:paladium. Images were obtained with a Philips EM-300 at 80 kV (23).

Electron microscopy of interphase nucleosomes

Size-fractionated chromatin fibres were isolated from chicken erythrocytes and prepared for electron microscopy as previously described (52, 53). Benzylalkyldimethylammonium chloride (BAC) (Sigma) was added to the chromatin to a concentration of 2 x 10-4 % (v/v). The mixture was incubated at RT for 30 mins. The chromatin was spread on formvar/carbon coated copper grids (TAAB). The grids were washed with ddH2O and 90% ethanol and allowed to dry. For contrast enhancement the grids were rotary-shadowed by a Leica ACE600 at a pressure of 1-2.5x10^-5 mbar. Rotating samples were coated with 2 nm platinum (measured by a quartz sensor) at an elevation angle of 7°. The grids were examined by a JEOL JEM-1400 Plus TEM, operated at a magnification of 20K, 80kV. Electron micrographs were acquired using GATAN OneView camera.

Indirect immunofluorescence

To analyse GFP:CENP-A localization an immuno-stain for CENP-T was performed. Cells were seeded onto Concanavaline A (ConA) coated coverslips and left to adhere for 1 hour in the incubator prior to fixation. Cells were washed with warm PBS and fixed with pre-warmed 4% formaldehyde/PBS solution for 10 minutes. Cells were permeabilised by incubating coverslips for 2 minutes in 0.15% Triton X-100/PBS solution. Cells were blocked in 1% BSA/PBS solution for 1 hour at room temperature and subsequently incubated with primary rabbit anti-GgCENP-T antibody diluted 1:1000 (14) in the blocking solution for 1 hour. Prior to secondary antibody incubation cells were washed three times in 0.1% Tween20/PBS solution. Fluorophore conjugated secondary antibody (Alexa Fluor 594; Jackson ImmunoResearch Laboratories, Inc.) was diluted 1:1000 in the blocking solution and the incubation 45 minutes long. Several washes followed and coverslips were finally mounted on slides using Vectashield containing DAPI (Vector Labs) as antifade media. 3D intact cell image stacks were deconvolved, quick projected and saved as tiff images.

SDS-PAGE and immunoblotting

Cell lysates were sonicated and boiled in sample buffer (5% sucrose, 1% SDS, 16.67 mM Tris-HCl pH 6.8, 0.67 mM EDTA, 10% β-Mercaptoethanol (v/v), 0.01% bromophenol blue). Lysates were resolved in SDS-PAGE with 12% polyacrylamide gels (BioRad electrophiresis apparatus). After transferring the proteins to a nitrocellulose membrane (Amersham, GE) blocking with 3% low fat milk in 0.05% Tween20/PBS solution for 1 hour

was performed prior immunoblotting. Primary antibodies used for immunoblotting included: mouse anti-αtubulin (1:5000, B512 Sigma), rabbit anti-GgCENP-A (1:1000) and rabbit anti-GFP (1:1000, Life Technologies). Membranes were washed in 0.05% Tween20/PBS solution and incubated with secondary antibodies (IRDye 800 or IRDye 680; Li-Cor Biosciences) and abundantly washed before proceeding to the detection using a CCD scanner (Odyssey; Li-Cor Biosciences). Quantification of CENP-A bands was performed using ImageJ and normalized for the tubulin signal.

SUPPLEMENTARY FIGURE LEGENDS:

Supplementary Figure 1. **Characterization of DT40 cells stably expressing GFP:CENP-A. A**. Western analysis of whole cell lysate prepared from DT40 cells stably expressing GFP:CENP-A or the wild type cell line (control). The membrane was probed with primary antibodies recognising CENP-A, tubulin and GFP. A LI-COR system was used for imaging. **B**. Indirect immunofluorescence of cells expressing GFP:CENP-A. Cells were probed with anti CENP-T antibody (red). Mitotic stages are indicated on the left of the panels. Scale bar, 5 μm. **C**. Representative image of DT40 cells stably expressing GFP:CENP-A where CENP-A signal co-localizes with CENP-T on unfolded fibres. Scale bar, 5 μm.

Supplementary Figure 2. **Increasing the number of bins increases the resolution of the histograms. A**. Two columns of frequency histograms containing fibre length data for interphase and mitotic samples. Columns show progressive improvements in the histogram resolution by adjusting the number of bins and bin width (bin width indicated in

brackets); 50 bins (200 nm), 60 bins (166 nm), 80 bins (125 nm) and 100 bins (100 nm). The scale on the y axis has been kept different for interphase and mitosis to allow a better visualization of the peaks in the two data sets. **B**. Frequency histograms containing both data sets allotted into 100 bins (100 nm) are merged together in one plot with the same scale on the y axis.

Supplementary Figure 3. **Quantification of the inter-nucleosome distance in interphase. A**. TEM of mitotic chromosomes centrifuged onto a carbon film after TEEN buffer treatment. The center-to-center distance between adjacent nucleosomes (n=203) was determined to be 20.4 ± 0.68 nm (mean ± SEM). The inset represent a 2 X zoom**.** Scale bar, 50 nm. **B**. Micrograph of interphase chromatin from chicken erythrocytes spread onto grids and imaged by TEM following rotary shadowing. The center-to-center distance between adjacent nucleosomes (n= 65) was determined to be 38.71 ± 1.6 nm (mean ± SEM). The inset represent a 2 X zoom. Scale bar, 50 nm. **C**. Schematic of the calculations used to predict the DNA content at the chicken centromere.

Supplementary Figure 4. **Characterization of DT40 conditional knockouts or deletion cell lines stably expressing GFP:CENP-A. A**. Indirect immunofluorescence of cells expressing GFP:CENP-A probed with anti CENP-T antibody (red). The localization of GFP:CENP-A is at the kinetochore in all the conditions analysed. Scale bar, 5 μm. **B**. Growth curves of mutant cell lines plus or minus doxycycline and DT40 control

cell line. **C.** Western blot of whole cell lysate of samples prior to the addition of doxycycline.

Supplementary Figure 5. **Characterization of CENP-N and CENP-W conditional knockouts or inducible auxin-degron for CENP-T cell lines stably expressing GFP:CENP-A. A**. Indirect immunofluorescence of cells expressing GFP:CENP-A and probed with anti CENP-T antibody (red). The localization of GFP:CENP-A is at the kinetochore in all the conditions analysed. Scale bar, 5 μm. **B**. Growth curves of mutant cell lines in the presence of doxycycline. The growth curves for AID-CENP-T:CENP-$T^{ON/OFF}$ cells plus and minus auxin are shown in (32), Figure 2C. These cells begin to die within 24 hours of the addition of auxin. **C.** Western blot of whole cell lysate of samples with no addition of doxycycline or auxin.

Supplementary Figure 6. **Quantification of CENP-A levels.** The quantification of the bands for endogenous CENP-A, GFP:CENP-A and tubulin from the blots shown in Figs. S4C (**A**) or Fig. S5C (**B**) was performed using ImageJ. The graphs show the levels of endogenous CENP-A (blue) and GFP:CENP-A (red) after normalization with tubulin.

Supplementary Figure 7. **Multi-peak analysis of centromere chromatin fibres unfolding data sets in CENP mutant cell lines.** For all the panels: the bottom part of each graph show probability density histograms, where x and y axes show frequency and centromere fibre length (μm) respectively; the data sets are divided in 100 bins (interphase and mitosis wild type – Figs. 2, S2) with a resolution of 100 nm or 50 bins (mutants) with a resolution of 200 nm per bin. Histograms of

centromere fibre length showing putative populations of fibre lengths within the data sets underlined by the diverse peaks (red lines). The scale on the y axis has been kept different for the different mutants to allow a better visualization of the peaks in the data sets. The best fitting curve is shown (blue line) for all the samples. Inset, fluorescent images of centromere fibres are shown for each mutant; DAPI, GFP and merge respectively. Scale bar, 1 μm. The upper part of each graph highlights the amount of residuals.

Supplementary Figure 8. **Centrochromatin unfolding analysis CENP-N, CENP-W and CENP-T depleted cells. A.** Schematic displaying the sub-populations of the peaks (μm) and the distance of the interval between two consecutive peaks (μm). Data obtained from multi-peak fitting analysis in panel B. **B**. For all panels: the bottom part of each graph show probability density histograms, where x and y axes show frequency and centromere fibre length (μm) respectively; the data sets are divided in 50 bins with a resolution of 200 nm per bin. Histograms of centromere fibre length showing putative populations of fibre lengths within the data sets underlined by the diverse peaks (red lines). The scale on the y axis has been kept different for the different mutants to allow a better visualization of the peaks in the data sets. The best fitting curve is shown (blue line) for all the samples. Inset, fluorescent images of centromere fibres are shown for each mutant; DAPI, GFP and merge respectively. Scale bar, 1 μm. The upper part of each graph highlights the amount of residuals.

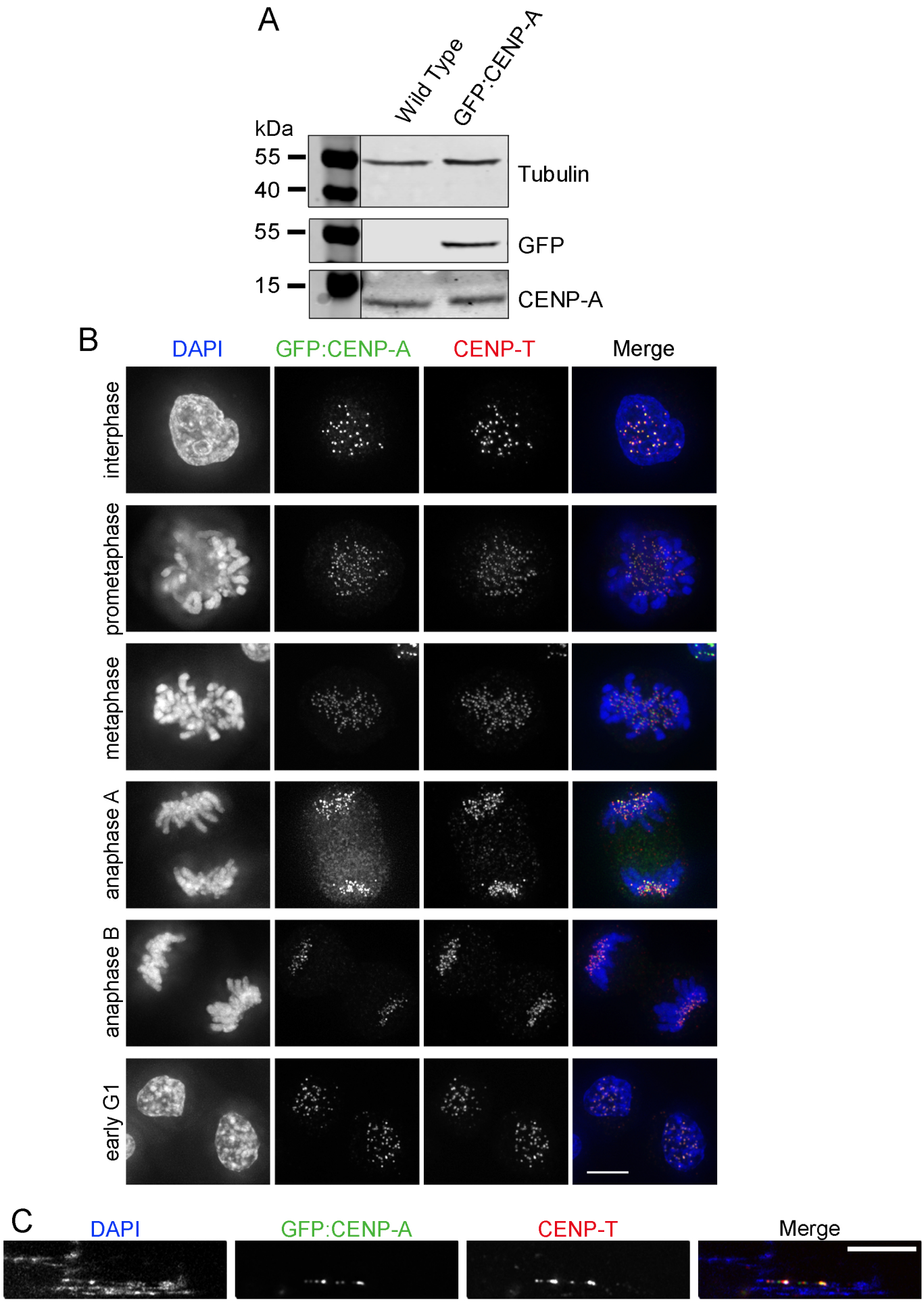
A
Wild Type
GFP:CENP-A
kDa
55
40
Tubulin
55
GFP
15
CENP-A
B
DAPI
GFP:CENP-A
CENP-T
Merge
interphase
prometaphase
metaphase
anaphase A
anaphase B
early G1
C
DAPI
GFP:CENP-A
CENP-T
Merge

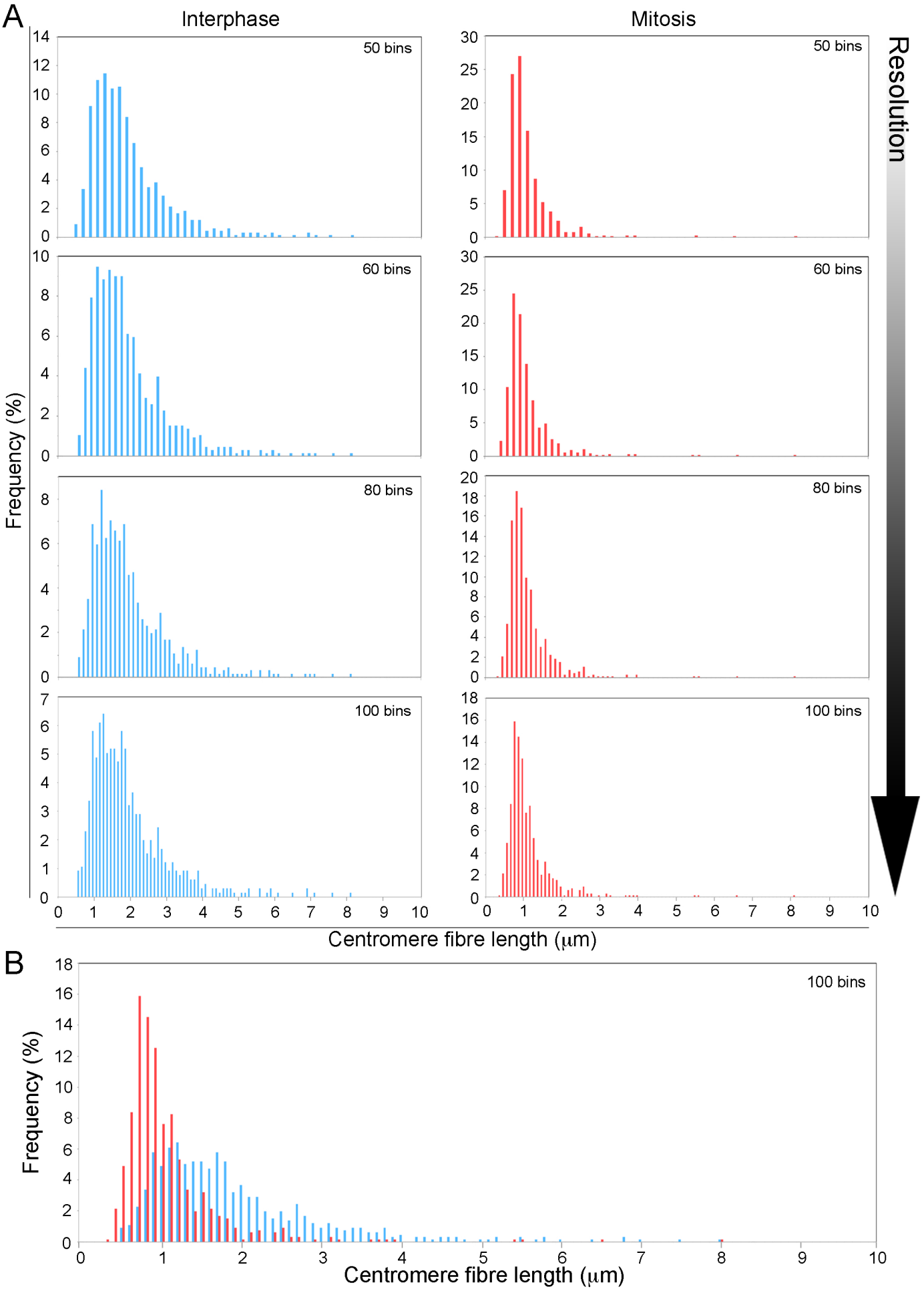
A
Interphase
Mitosis
50 bins
60 bins
80 bins
100 bins
Frequency (%)
Resolution
Centromere fibre length (μm)
B
100 bins
Frequency (%)
Centromere fibre length (μm)

A

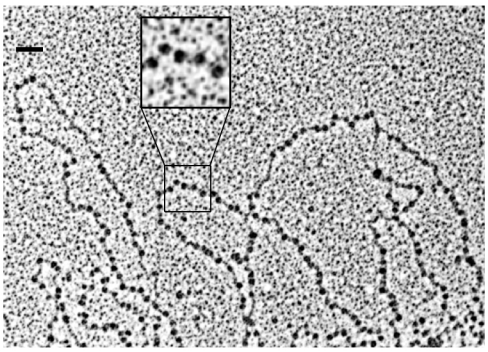

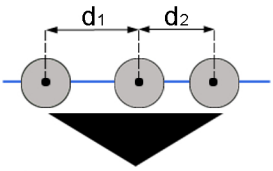

$\bar{d}$ = 20.43 ± 0.68 nm

B

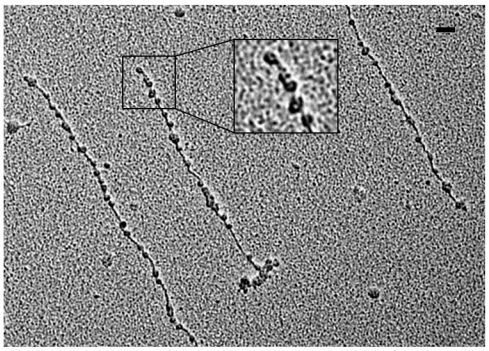

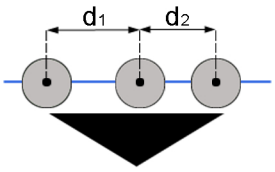

$\bar{d}$ = 38.71 ± 1.6 nm

C

INTERPHASE: **690 nm** ÷ **38.71 nm** = **17.8 nucleosomes** x **5 layers** = **89 nucleosomes**

MITOSIS: **835 nm** ÷ **20.43 nm** = **40.8 nucleosomes** x **3 layers** = **122.4 nucleosomes**

Mean step of unfolding | internucleosome distance | per layer | sub-populations of unfolded fibers | total in the DT40 centromere

89 nucleosomes x **200 bp** = **17.8 Kbp DNA in centromere**

122.4 nucleosomes x **200 bp** = **24.4 Kbp DNA in centromere**

total in the DT40 centromere | ~ DNA + linker on a nucleosome

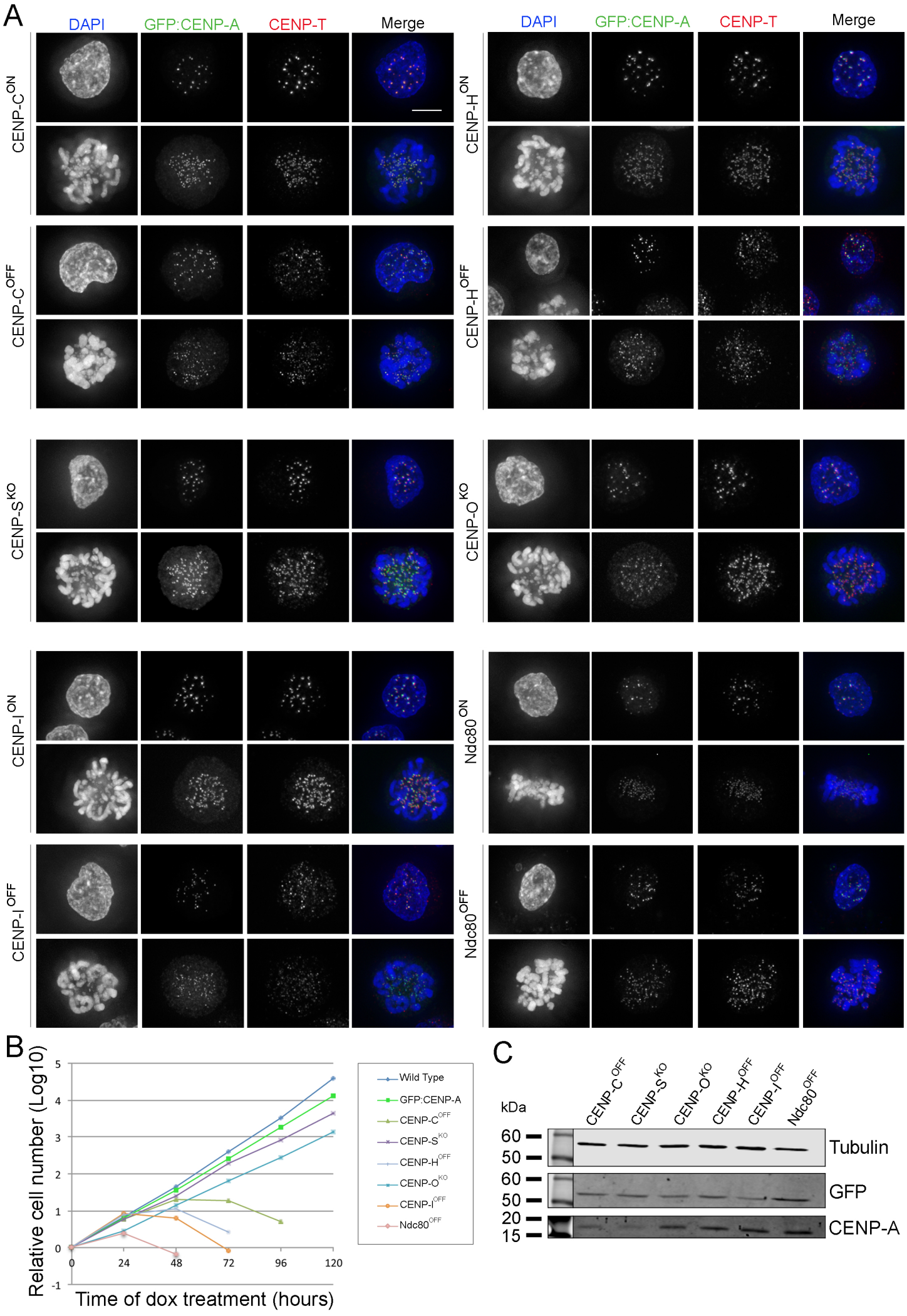
A
DAPI
GFP:CENP-A
CENP-T
Merge
CENP-C^ON
CENP-H^ON
CENP-C^OFF
CENP-H^OFF
CENP-S^KO
CENP-O^KO
CENP-I^ON
Ndc80^ON
CENP-I^OFF
Ndc80^OFF
B
Relative cell number (Log10)
Time of dox treatment (hours)
0
24
48
72
96
120
-1
0
1
2
3
4
5
Wild Type
GFP:CENP-A
CENP-C^OFF
CENP-S^KO
CENP-H^OFF
CENP-O^KO
CENP-I^OFF
Ndc80^OFF
C
kDa
CENP-C^OFF
CENP-S^KO
CENP-O^KO
CENP-H^OFF
CENP-I^OFF
Ndc80^OFF
60
50
60
50
20
15
Tubulin
GFP
CENP-A

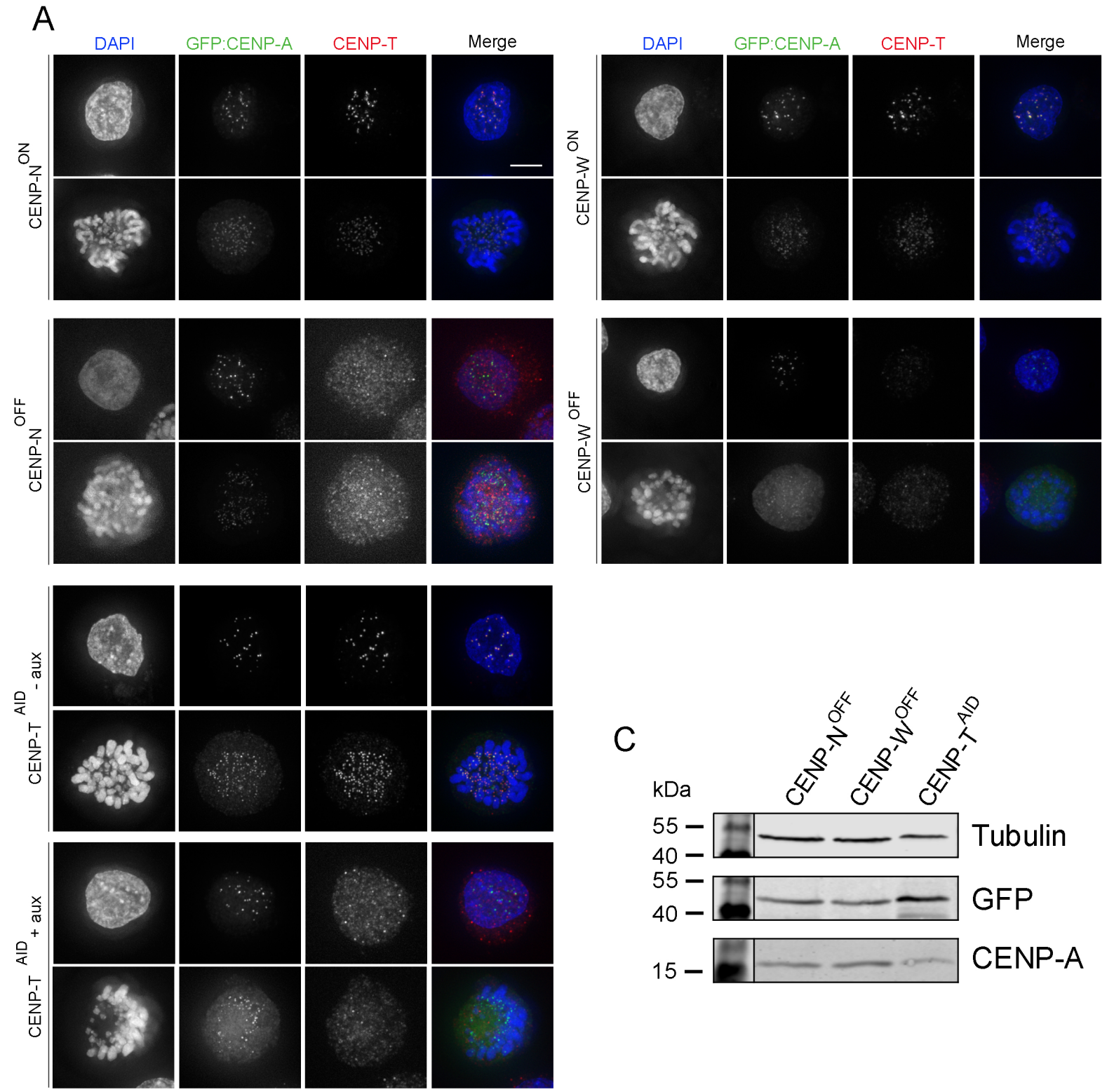
A
DAPI
GFP:CENP-A
CENP-T
Merge
CENP-N ON
CENP-W ON
CENP-N OFF
CENP-W OFF
CENP-T AID - aux
CENP-T AID + aux

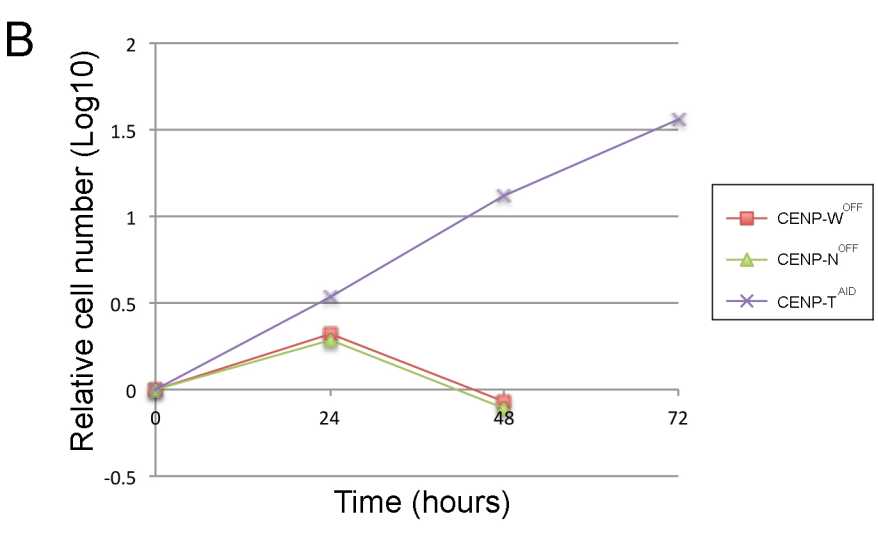
B
Relative cell number (Log10)
2
1.5
1
0.5
0
-0.5
0
24
48
72
Time (hours)
CENP-W OFF
CENP-N OFF
CENP-T AID

C
CENP-N OFF
CENP-W OFF
CENP-T AID
kDa
55
40
55
40
15
Tubulin
GFP
CENP-A

A

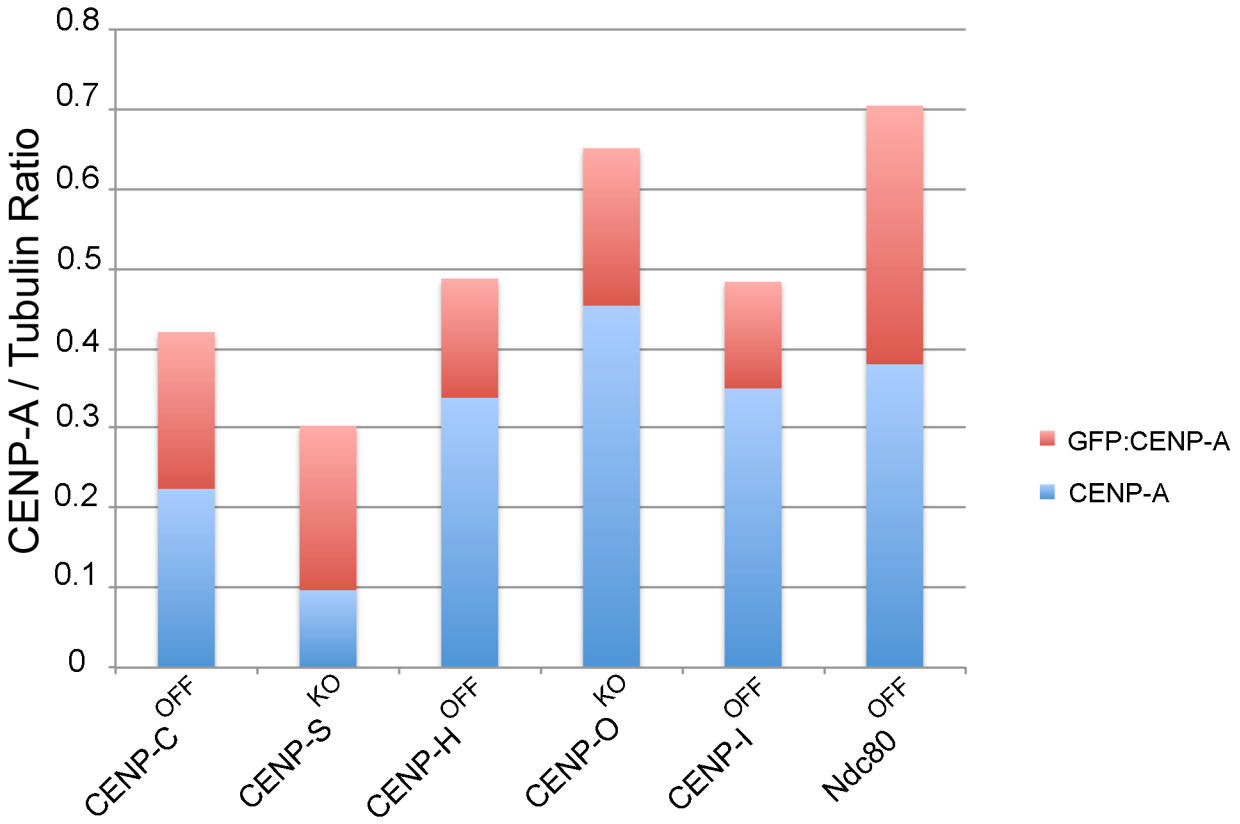
0.8
0.7
0.6
0.5
0.4
0.3
0.2
0.1
0
CENP-A / Tubulin Ratio
CENP-C OFF
CENP-S KO
CENP-H OFF
CENP-O KO
CENP-I OFF
Ndc80 OFF
GFP:CENP-A
CENP-A

B

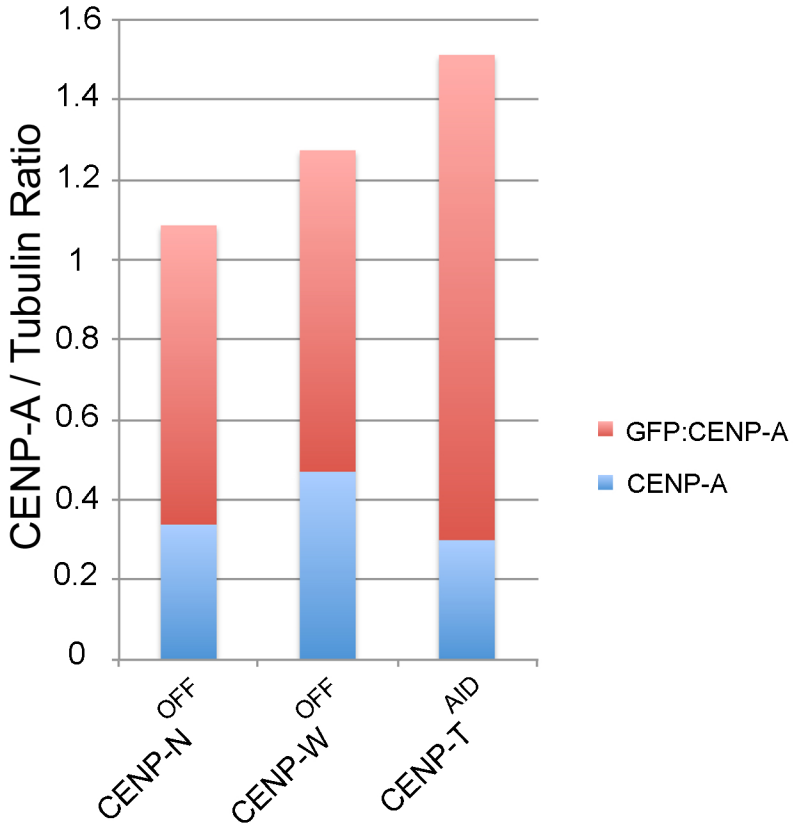
1.6
1.4
1.2
1
0.8
0.6
0.4
0.2
0
CENP-A / Tubulin Ratio
CENP-N OFF
CENP-W OFF
CENP-T AID
GFP:CENP-A
CENP-A

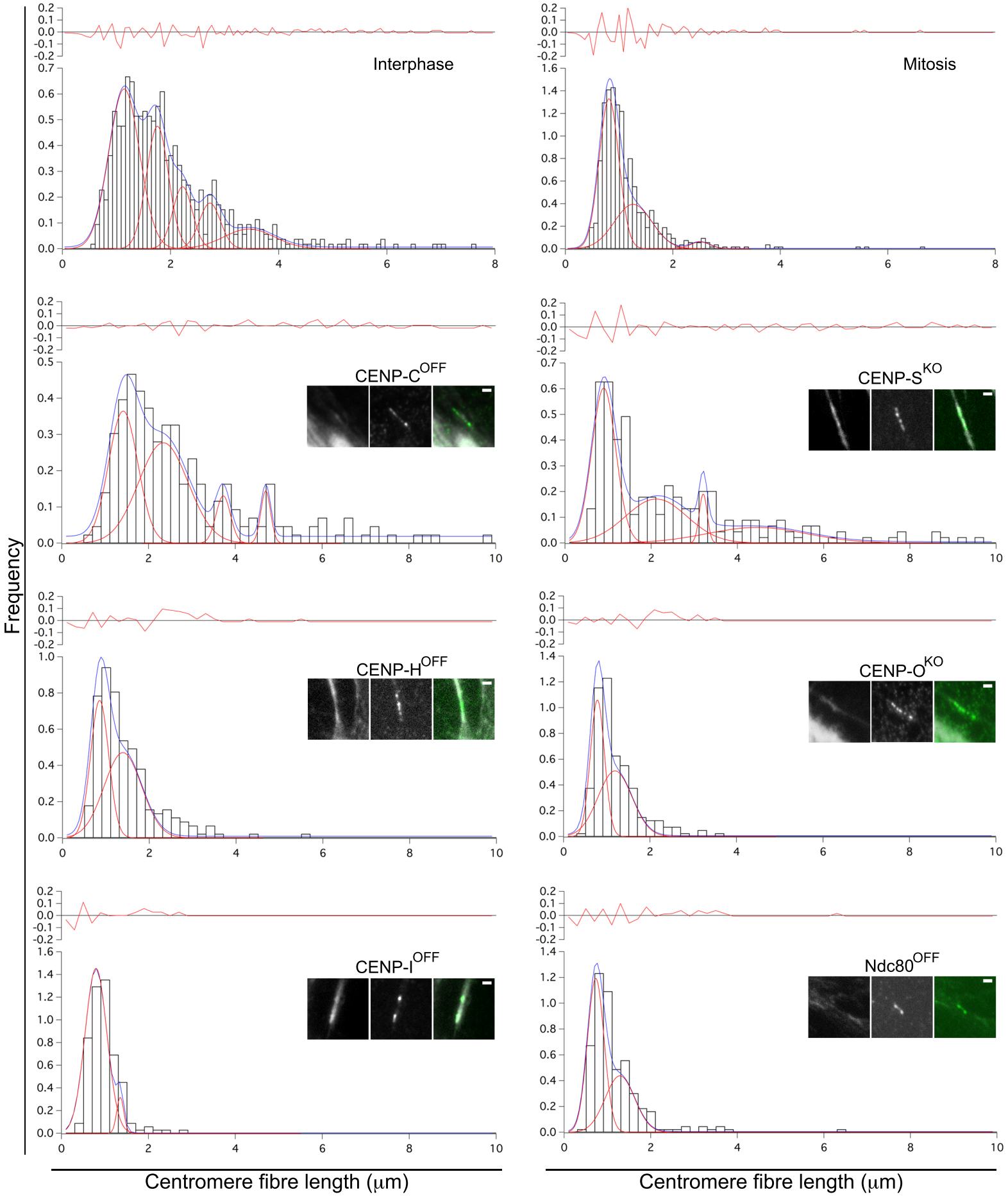
Interphase
Mitosis
CENP-C^OFF
CENP-S^KO
CENP-H^OFF
CENP-O^KO
CENP-I^OFF
Ndc80^OFF
Frequency
Centromere fibre length (μm)
Centromere fibre length (μm)

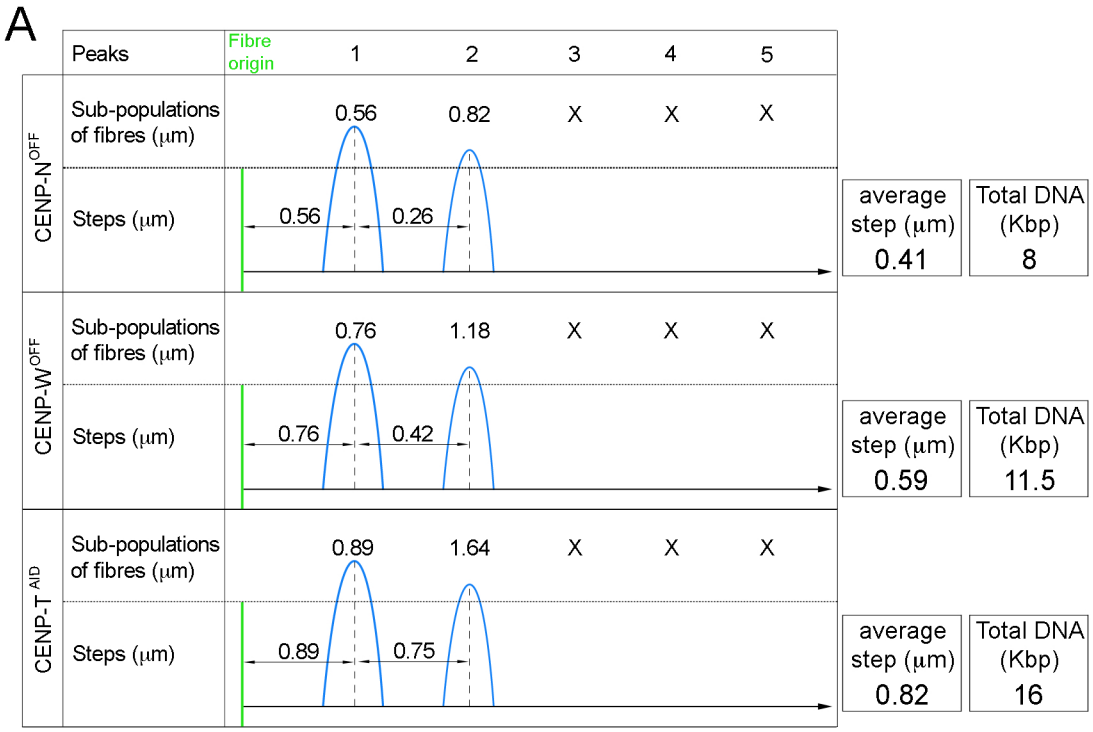
A
Peaks
Fibre origin
1
2
3
4
5
CENP-N^OFF
Sub-populations of fibres (μm)
0.56
0.82
X
X
X
Steps (μm)
0.56
0.26
average step (μm)
0.41
Total DNA (Kbp)
8
CENP-W^OFF
Sub-populations of fibres (μm)
0.76
1.18
X
X
X
Steps (μm)
0.76
0.42
average step (μm)
0.59
Total DNA (Kbp)
11.5
CENP-T^AID
Sub-populations of fibres (μm)
0.89
1.64
X
X
X
Steps (μm)
0.89
0.75
average step (μm)
0.82
Total DNA (Kbp)
16

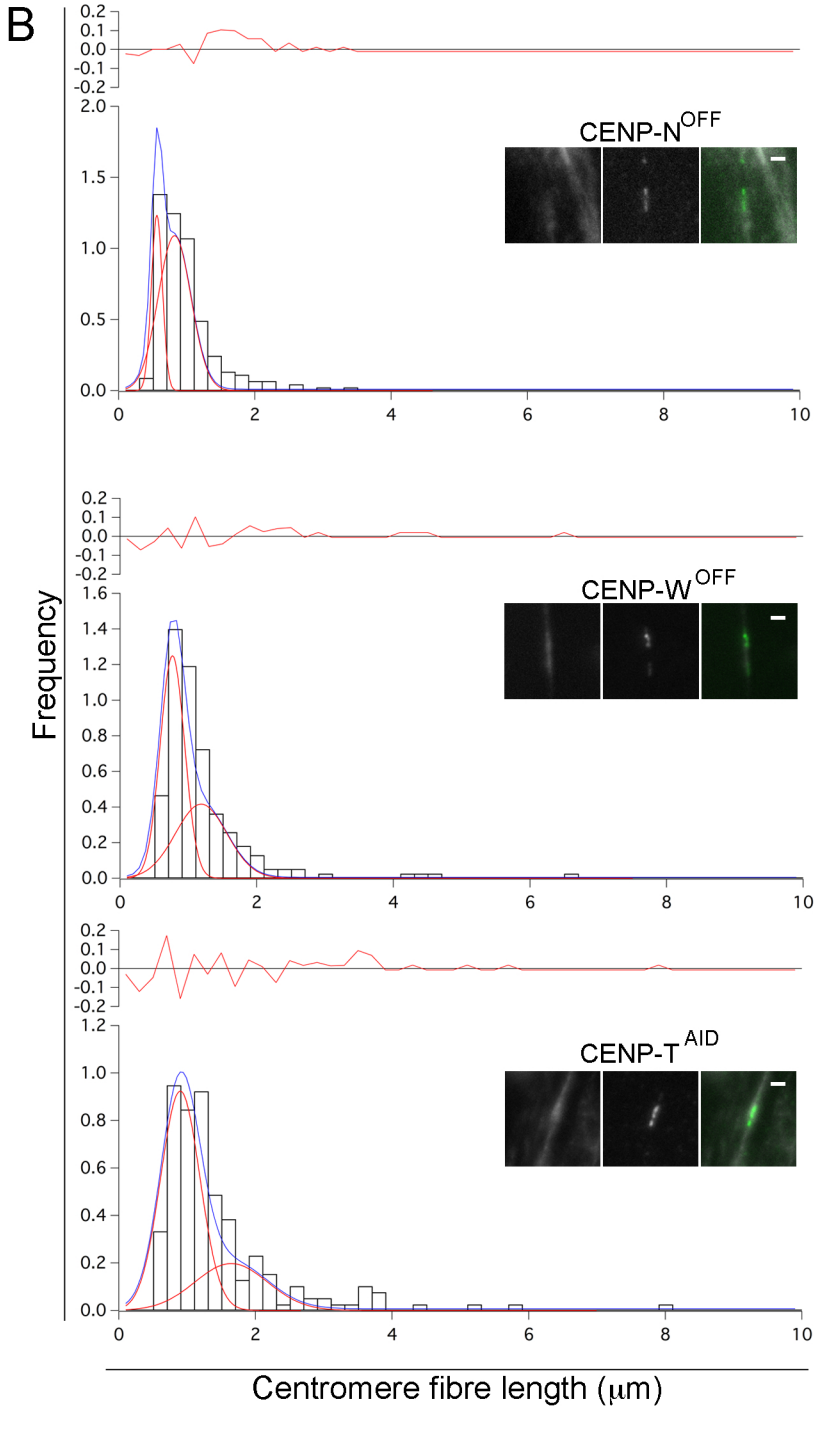
B
CENP-N^OFF
CENP-W^OFF
CENP-T^AID
Frequency
Centromere fibre length (μm)